Scientific paper

Combined Application of MMT K10 Supported Copper Oxide Nanoparticles for Complete Removal of Cr(VI) from Aqueous Solution and their Antibacterial Potential

Mahesh Kumar Gupta,* Praveen Kumar Tandon, Mubashra Afroz and Saumya Agrahari[1]

Department of Chemistry, University of Allahabad, Prayagraj-211002, India

** Corresponding author: E-mail: mahesh27620@gmail.com*

Received: 11-27-2020

Abstract

Montmorillonite K10 (MMT K10) supported copper oxide nanoparticles (CuONPs) were synthesized by incorporating CuONPs onto the surface of MMT K10 by reducing the metal precursor with the help of hydrazine hydrate. Effects of various factors on the efficiency of composite to remove hexavalent chromium were studied to find out the optimum conditions for maximum removal. Under optimum conditions 15 mg of the synthesized nanocomposite was found capable to almost completely remove (99.9%) hexavalent chromium in 30 min from a 10 ppm aqueous chromium solution and that too in a wide range of pH from 2.88 to 5.56. The synthesized MMT K10 supported CuONPs were characterized by UV, SEM-EDX, FTIR and XRD studies. The average particle size of supported CuONPs was found to be 22.9 nm. Antibacterial potential of the prepared composite was also studied for one Gram-positive bacterium *Staphylococcus aureus* (ATCC 25323) and one Gram-negative bacterium *Pseudomonas aeruginosa* (ATCC 27853). The prepared nanocomposite was found to have excellent bactericidal potential and its statistical analysis was performed using *t*-test which indicates both bacterial strains of *Pseudomonas aeruginosa* and *Staphylococcus aureus* show different zone of inhibition for different concentrations.

Keywords: Montmorillonite K10; CuONPs; hydrazine hydrate; hexavalent chromium; bactericidal potential

1. Introduction

Recently water pollution due to heavy metals ions has become a serious concern because metal ions are non-biodegradable, accumulate easily in the environment and even in a low concentration cause adverse health hazards.[1] Presence of chromium in the effluents coming from paint, metal finishing, textile and dyeing, electroplating, and leather tanning industries[2] is of considerable concern due to its highly toxic, carcinogenic and mutagenic nature. It also has adverse effect on plant and animal tissues even at low concentrations.[3–5] Out of many, Cr(III) and Cr(VI) are the most stable oxidation states which are much different in their chemical and toxicological properties. Cr(VI) is more hazardous than Cr(III) species due to its greater water solubility, mobility and bio-accessibility.[6,7] Toxicity of trivalent chromium toward a living cell is 500–1000 times less than hexavalent chromium.[8] Exposure to chromium(VI) causes liver damage, pulmonary congestion, oedema, skin irritation and ulcer.[9]

Out of many techniques proposed for the removal of chromium(VI) from wastewater the extensively used techniques include chemical precipitation, ion exchange, coagulation, reverse osmosis, electrolysis, membrane process, chemical reduction, photocatalytic oxidation, evaporation and biosorption process.[10–15] All these methods have limitations in the sense that they often involve high capital and operational costs, require high energy consumption, and may produce secondary pollutants. Adsorption method has been found to be an attractive technique for the removal of pollutants from wastewater because of its flexibility and simplicity of design, cost effectiveness, eco-friendliness and high efficiency compared to other conventional methods. In addition, adsorption does not generate hazardous substances and avoids the secondary pollution. Due to all these properties adsorption technique has been

extensively applied for the removal of heavy metal ions from wastewater.[16–18]

Metallic nanoparticles have been extensively studied to be used to decontaminate aqueous solutions as compared to conventional adsorbents due to their nanosize which increases the surface area resulting in greater efficiency, faster rate of adsorption and easier separation after adsorption. Metal-based NPs have been found useful in antiviral, antibacterial, antifouling, and antifungal applications also.[19,20] Antibacterial activity of nanoparticles has been widely studied for human pathogenic bacteria *Pseudomonas aeruginosa* and *Staphylococcus aureus*. *Pseudomonas aeruginosa* is a multidrug-resistant pathogen known for its broad spectrum affecting both plants and animals and its infection mainly spreads during hospitalization, similar to ventilator-associated pneumonia and various sepsis syndromes while *Staphylococcus aureus* frequently found in the upper respiratory tract and on the skin. It can adapt to extreme changes in external oxygen concentration, able to grow even in the absence of oxygen and responsible for causing skin infections including abscesses, respiratory infections such as sinusitis, and food poisoning.[21]

The bactericidal property of nanoparticles depends on their size, shape, stability, and concentration added to the growth medium. Bacterial cell size usually lies in micrometer dimension, with pores of nanometer dimension in their outer cellular membranes. Nanoparticles having size less than that of pore size of the bacterial cell membrane, have a unique property of crossing the cell membrane and restrict bacterial growth.[22] Cu and CuO nanoparticles were analyzed as a plausible antibacterial agent for many pathogenic species like *E. coli*, *Bacillus subtilis*, *Vibrio cholera*, *Pseudomonas aeruginosa*, *Syphilis typhus*, and *Staphylococcus aureus*.[23] Addition of silver nanoparticles imparts antimicrobial properties in household products[24,25] and growth of *Escherichia coli* and *Bacillus subtilis* is inhibited by adding copper nanoparticles (CuNPs)[26,27] probably due to interactions with -SH groups leading to protein denaturation.[28] Copper also shows a dual capacity to act as a cofactor and biocatalyst with a critical balance for proper intracellular metal homeostasis and metabolism.[29,30] Metal oxide nanoparticles are 7–50 times less toxic towards mammalian cells compared to ionic forms of respective metals.[9] CuO nanoparticles show excellent antibacterial activity against *Klebsiella pneumoniae, Pseudomonas aeruginosa*, *Salmonella paratyphi* and *Shigella* strains,[31] reduce (99.9%) concentrations of *E. coli* and *S. aureus* after 24 h of incubation.[32] CuO nanoparticles synthesized with a *Streptomyces* species[33] and naturally obtained gum karaya[23] showed excellent reduction of *E. coli, S. aureus, and Aspergillus niger*. Polyaniline coated Cu_2O nanoparticles[34] and have been found to be effective against Gram-positive and Gram-negative bacteria.[22]

Difference in the outermost protective covering of Gram-positive and Gram-negative bacteria may also be a reason for their changed response towards various bactericidal agents. Vast majority of bacteria follow the color differentiation by giving different staining intensity by the Gram technique and this leads to classify bacteria in two major groups, Gram-negative and Gram-positive bacteria. In Gram staining the decolorizing step with alcohol washes the primary stain (crystal violet) from the cells and the secondary stain colors the bacteria red. In contrast Gram-positive bacteria are covered with strong and thick cell walls which do not allow the crystal violet to be removed and thus remain purple.[35] There are many distinguishing features between the Gram-positive and Gram-negative bacteria. Characteristic feature for both classes is that their cytoplasmic membrane is surrounded by a cell wall. Periplasm contains a wide variety of ions and proteins that are needed for numerous functions involving cellular (electron) transport, substrate hydrolysis, degradation and detoxification.

In Gram-negative bacteria the periplasm occupies the space between the plasma membrane and the outer membrane. Existing above the plasma membrane and the outer membrane the periplasm is an integral compartment of the gram-negative cell wall.[36] Outer membrane, peptidoglycan layer, and periplasm along with plasma membrane constitute the gram-negative envelope.[36,37] The presence of the outer membrane in Gram negative bacteria next to the periplasmatic space is the major difference between those bacterial classes as it does not exist in Gram-positive bacteria. This outer membrane is a lipid bilayer, where the inner leaflet is composed of phospholipids and the outer leaflet of lipopolysaccharides.[38] In both families, the cell wall contains peptidoglycan layers that stabilize the cell membranes. The cell wall of Gram-positive bacteria is made of many peptidoglycan layers of about 40–80 nm that is much thicker than the single layered 7–8 nm thick cell wall of Gram-negative bacteria.[39] Therefore, the periplasmic space between the inner and outer membrane in Gram-negative bacteria is much larger than the narrow periplasm of Gram-positive bacteria. Also specific for Gram-positive bacteria is the occurrence of teichoic acid in the cell wall that can be linked via a glycolipid anchor with the plasma membrane. Gram-positive bacteria have larger fraction of negatively charged phosphatidylglycerol whereas Gram-negative bacteria contain larger proportions on zwitterionic phosphatidylethanolamine in addition to phosphatidylglycerol. Presence of different charges on the surface may influence the bactericidal potential also. Peptidoglycan, due to its rigidity determines the strength and cellular shape of bacteria and accounts for around 90% of dry weight in Gram-positive and 10% in Gram-negative bacteria.

To obtain better capacity to remove chromium(-VI) from the contaminated water copper oxide nanoparticles, synthesized with the help of hydrazine hydrate, were supported on MMT K10. Montmorillonite K10 was selected as a supporting material due to its unique properties of

cation exchange and swelling ability in addition to its low cost and eco-friendly nature. It was also observed that copper oxide nanoparticles supported on MMT K10 showed excellent capacity to remove chromium(VI) from the contaminated water compared to the unsupported ones. The interlayer space of montmorillonite provides a very good platform to accommodate the nanoparticulates. Prepared copper oxide nanoparticles were characterized with the help of SEM-EDX, XRD and FTIR spectroscopy. Antibacterial nature of the nanocomposite for one Gram-positive bacterium *Staphylococcus aureus* (ATCC 25323) and one Gram-negative bacterium *Pseudomonas aeruginosa* (ATCC 27853) was also studied. Statistical analysis of two-tailed *t*-test was also performed to show bacteria have different zone of inhibition at different concentrations.

2. Experimental

2. 1. Materials and Methods

To get the solutions of desired strengths the stock solutions of $K_2Cr_2O_7$ and $CuSO_4.5H_2O$ (Merck) were diluted with double distilled water. Montmorillonite K10 (Sigma-Aldrich) was of the highest purity. All other chemicals like hydrazine hydrate, 1,5-diphenylcarbazide (LobaChemie), H_2SO_4, HCl and NaOH (Merck), Luria bertani broth, miller (SRL) and agar-agar (Fisher Scientific) were of Analytical grade or chemically pure substances which were used without further purification.

2. 2. Preparation of Clay-Supported Copper Oxide Nanocomposites (CuONC)

500 mg montmorillonite K10 was added to 10 mL (0.10 M) copper sulphate solution and after heating the solution to 60 °C for 20 min, hydrazine hydrate (0.5 mL) solution was added drop-wise over 5 min with constant stirring. Change in the colour of solution from blue-brown to black[40] indicates the formation of copper nanoparticles which in the presence of dissolved oxygen in water get oxidized to copper oxide nanoparticles. It is important to mention here that addition of 0.5 mL hydrazine hydrate to 10 mL copper sulphate solution of the mentioned strength is necessary for getting the best results. Deviation of this ratio decreases the removal efficiency of the composite. It was observed that increase in the amount of hydrazine hydrate results in the appearance of precipitate in the solution while if the lesser amount is added then proper colour change is not observed. Stirring was continued for an additional 60 min. UV-Vis spectrum of the solution showed two peaks, one of the peak is situated at 243 nm while the other one at 630 nm. The peak situated at 243 nm is due to the Cu_2O shell layer of the Cu-Cu_2O (Copper core-copper oxide shell nanoparticles) while that of peak around 630 nm correspond to the conversion of upper shell layers of the Cu_2O into more thermodynamically stable CuO layers. Appearance of the peaks in solution (Figure 1) confirmed[41,42] the formation of MMT K10 supported CuONPs.

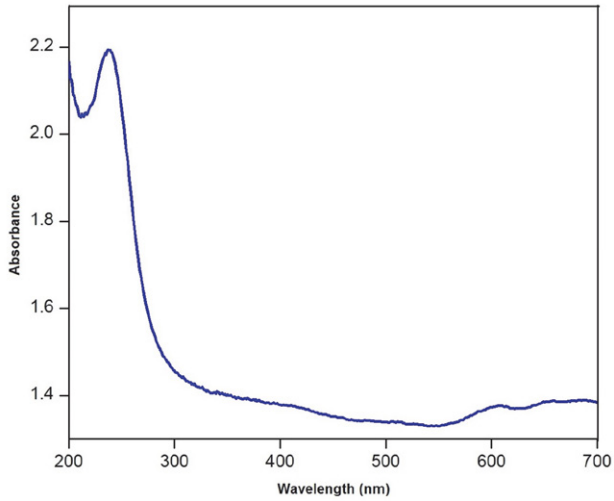

Figure 1: UV-Visible spectra of CuONPs

2. 3. Instrumentation and Measurement of Chromium

The amount of Cr(VI) remaining in the filtrate was measured with a double beam spectrophotometer (Systronics 2203). Standard solutions of NaOH and HCl were used to maintain the desired pH of the solution which was measured along with temperature with a digital pH meter (μ-pH System 361, Systronics). IR spectra were recorded on a spectrum 2 Perkin Elmer spectrophotometer version 10.4.00 FTIR spectrophotometer. SEM analysis was carried out using a JEOL (JSM 6490 LV) scanning electron microscope equipped with EDAX after coating the samples with platinum to investigate the morphological changes in MMT K10 before and after being loaded with CuONPs. Powder X-ray diffraction (PXRD) analysis was carried out using Rigaku Smart lab 3KW to obtain structural information. The surface areas of samples under varying conditions were calculated using a WT Classic Brunaur, Emmett and Teller (BET) surface area analyzer, WAKO, New Delhi India. Luria-Bertani (LB) agar solution was autoclaved with Vertical Autoclave (Metrex), all plating and inoculations were done inside a Vertical Laminar Air Flow (Impact Icon Instruments Company) and inoculated plates were incubated inside BOD Incubator (Metrex Scientific Instruments).

2. 4. Analysis of Remaining Cr(VI) By 1,5-Diphenylcarbazide (DPC) Method

In solution phase Cr(VI) strongly complexes with 1,5-diphenyl carbazide to give a dark pink chromium-diphenyl carbazide complex which absorbs strongly at 540

nm.[43] Stock solution of diphenyl carbazide was prepared by dissolving 250 mg of 1,5-diphenyl carbazide in 50 mL acetone and the solution was kept at 5 °C in freezer. In a typical procedure the calculated concentration of Cr(VI) solution mixed with 0.8 ml of H_2SO_4 (6N) and 1 mL DPC was diluted up to mark in a 25 mL flask. Solution was left for 10 min to develop the colour of Cr-DPC complex, intensity of which depends on the concentration of Cr(VI) in solution. Thus the remaining concentration of Cr(VI) is determined directly with the help of a standard calibration graph plotted between concentration vs. absorbance.

$$\% \text{ removal of contaminant} = \frac{C_i - C_f}{C_i} \times 100$$

where C_i and C_f are initial and final concentrations of contaminant

Stock solution of $K_2Cr_2O_7$ was diluted with double distilled water to get the solutions of desired concentrations. Calculated amount of MMT K10 supported CuNPs (MMT-CuNPs) was added to the stirred solution of Cr(VI). Stirring was continued for a fixed time and then the solution was filtered. Remaining Cr(VI) in the solution was measured with DPC method. To find out the optimum conditions effects of duration of treatment, amount of CuONC, pH, and initial Cr(VI) concentration were studied by changing the variables one by one keeping other factors constant. In all the cases, 10.0 mL of 0.1 M $CuSO_4$ $5H_2O$ and 0.5 mL of hydrazine hydrates were mixed. All experiments were conducted at room temperature.

2. 5. Antibacterial Activity

Gradual increase of resistance in microorganisms against drugs has increased the interest for the synthesis and utilization of novel antimicrobial metal nanoparticles.[44] Using disc diffusion method antibacterial activity of synthesized CuONPs against *Staphylococcus aureus* (ATCC 25323) and *Pseudomonas aeruginosa* (ATCC 27853) bacteria was studied. In all cases, 10.0 mL of 0.1 M $CuSO_4 \cdot 5H_2O$ solution and 0.5 mL of hydrazine hydrates were mixed for the synthesis of CuONPs. Different molar concentrations of 40 mg/mL, 60 mg/mL, 80 mg/mL, and 100 mg/mL of CuONPs were used to determine the zone of inhibition of aforementioned bacterial strains. Control experiments were carried out in the presence of DMSO solvent. Experiments were performed after sterilizing all the equipment and Luria Bertani agar solution in an autoclave at 121 °C for at least 15 minutes under the pressure of 15 psi. For preparation of Luria Bertani agar solution, 2.5 gm of Luria Bertani Broth, Miller and 2 gm of agar-agar were mixed in 100 ml of distilled water thoroughly and then autoclaved. In brief, 20 ml of Luria-Bertani agar solution (pH 7.2 at 60 °C) was poured onto the petriplates and then put to solidification for 20 minutes. The wells were made by using 5 mm gauge which were punched out in petriplates. With the help of micropipette, different concentrations of CuONPs samples i.e., 40 mg/mL, 60 mg/mL, 80 mg/mL, 100 mg/mL were poured into the wells on all petriplates. The petriplates were incubated at 37 °C for 24 h. The size of zone of inhibition was measured by ruler.

3. Results and Discussion

3. 1. Factors Affecting the Removal of Hexavalent Chromium

In order to find out the optimum conditions for maximum removal of Cr(VI) various factors affecting the removal were changed one by one keeping other conditions constant. Result of the change of time of treatment on the removal efficiency is given in Table 1(entries 2–6) and Figure **2A**. Constancy in the efficiency of removal of contaminant at later stages may be due to the relative sizes of contaminant and pores if the size of contaminant is small then stirring for longer duration may not be able to expel the particles from the pores. This may be due to the attainment of the saturation point on achieving almost complete removal. pH of the chromium solution was maintained with the help of standard solutions of sulphuric acid and sodium hydroxide. Removal efficiency of the composite remains constant from pH 2.56 to 5.6 but later on the removal efficiency decreases (Table 1, entries 7 to 10 and 5; Figure **2B**). Probably after a particular pH surface of MMT K10 becomes negatively charged and electrostatic repulsion between the negatively charged surface and the contaminants decreases the efficiency of the composite to remove the contaminants. Effect of increase in the concentration of Cr(VI) sample on the removal efficiency shown in Figure **2C** (Table 1, entries 11 to 14 and 5) may be because of the reason that further increase in the concentration of contaminants beyond the capacity of a particular amount of composite having fixed active sites will not affect the removal and the excess ions of the contaminant will remain in the solution thus decreasing the percentage of removal. It was observed that increase in the amount of nanocomposite increases the removal efficiency till almost complete removal of chromium is obtained (Table 1, 15 to 18 and 5; Figure **2D**). Effect of change of the amount of HH on the removal efficiency (Table 1, entries 19 to 22 and 4; Figure **2E**) may be considered in conjunction with the effect of change of pH of the medium. Initial increase in the amount of HH increases the number of nanoparticles formed which increase the removal efficiency till a maximum is obtained for a fixed amount of copper sulphate. Addition of further HH increases pH of the medium and results of change of pH of the medium clearly show that increase in pH above the optimum value has a negative effect on the efficiency of removal. To determine the effect of loading of CuONC on the solid support, ratio of the amounts of copper sulphate and hydrazine hydrate

Table 1: Effect of various factors on the removal of Cr(VI) from contaminated water (In all the cases 25.0 mL Cr(VI) solution was taken)

S. No.	Time (min)	pH	Conc (ppm)	Amount of nano-composite	Volume of H.H	Reaction volume [$CuSO_4$ $5H_2O$+ H.H] (mL)	Amount of MMT K 10 (mg)	% removal
1.	30	5.56	10	–	–	–	15	11.0
2.	05	5.56	10	15	0.5	10 + 0.5	500	73.3
3.	10	5.56	10	15	0.5	10 + 0.5	500	85.0
4.	20	5.56	10	15	0.5	10 + 0.5	500	98.0
5.	30	5.56	10	15	0.5	10 + 0.5	500	99.9
6.	40	5.56	10	15	0.5	10 + 0.5	500	99.8
7.	30	2.58	10	15	0.5	10 + 0.5	500	99.8
8.	30	4.58	10	15	0.5	10 + 0.5	500	99.8
9.	30	7.59	10	15	0.5	10 + 0.5	500	93.0
10.	30	10.52	10	15	0.5	10 + 0.5	500	11.0
11.	30	5.56	02	15	0.5	10 + 0.5	500	99.5
12.	30	5.56	05	15	0.5	10 + 0.5	500	99.5
13.	30	5.56	15	15	0.5	10 + 0.5	500	92.0
14.	30	5.56	20	15	0.5	10 + 0.5	500	89.0
15.	30	5.56	10	05	0.5	10 + 0.5	500	32.5
16.	30	5.56	10	10	0.5	10 + 0.5	500	77.9
17.	30	5.56	10	12	0.5	10 + 0.5	500	91.8
18.	30	5.56	10	18	0.5	10 + 0.5	500	99.8
19.	30	5.56	10	15	0.2	10 + 0.5	500	80.0
20.	30	5.56	10	15	0.3	10 + 0.5	500	86.0
21.	30	5.56	10	15	0.4	10 + 0.5	500	93.5
22.	30	5.56	10	15	0.6	10 + 0.5	500	99.1
23.	30	5.56	10	15	0.5	4.0 + 0.2	500	38.3
24.	30	5.56	10	15	0.5	6.0 + 0.3	500	51.3
25.	30	5.56	10	15	0.5	8.0 + 0.4	500	80.6
26.	30	5.56	10	15	0.5	12 + 0.6	500	98.1

was varied (Table 1, entries 23 to 26 and 5; Figure **2F**). It was observed that use of 10.0 mL of copper sulphate mixed with 0.5 mL of hydrazine hydrate with addition of 500.0 mg of MMT K10 gave the best results. It may be mentioned that proper colour change was not observed if the ratio of HH and copper sulphate was decreased from 1:20, while formation of suspended particles takes place if the ratio is increased. Proper formation of CuONPs takes place only when 0.5 mL of HH was used to reduce 10 mL (0.1 M) solution of copper sulphate. Maximum yield of 99.9 % for Cr(VI) was obtained only when 1:20 ratio is maintained. Coming to the control experiment negligible (11%) removal of chromium(VI) was observed (Table 1, entry 1) when the experiment was performed only by adding MMT K10 in the contaminated water. This indicates that the clay mineral mainly helps in preventing the agglomeration of CuONPs prepared during the process and has no role in the removal of Cr(VI) from the contaminated water.

3. 2. Powder X-Ray Diffraction Pattern Study

Powder X-ray diffraction patterns of pure MMT K10 and MMT K10 supported CuO nanoparticles are shown in Figure 3. Peaks at 2θ = 20.95 and 26.60 obtained in pure MMT K10 are due to quartz impurity.[45] In MMT K10 supported CuO nanoparticle peaks at 32.70, 35.48, 53.8, 61.8 are due to crystalline CuO which correspond well with the (110), (110), (020) and (–113) planes of the monoclinic copper(II) oxide phase (tenorite, ICSD #01-089-2529).[46] The average size of MMTK10 supported CuO nanoparticles was found to be 22.9 nm which was calculated by using the Debye-Scherrer equation.

$$D = \frac{0.9 \times \lambda}{\beta \times Cos\,\theta}$$

Where D shows crystallite size, λ- wavelength and β- peak width (FWHM).

3. 3. Scanning Electron Microscopy-Energy Dispersive X-ray Analysis

SEM analysis of pure MMT K10 (Figure **4A**) shows asymmetrical particles while EDX spectrum (Figure **4B**) shows Si, O, Al and Mg as the main constituent in decreasing order of concentration.[47] SEM and EDX given in Figure **4C** and **4D** clearly shows that the irregular shape of CuONPs particles are accommodated on MMT K10 surface. The study also confirmed that the synthesized nanoparticles are supported on the surface of the MMT K10 by integration of metal in interlayer present on MMT K10 and are stabilized by the electronic alterations and Vander

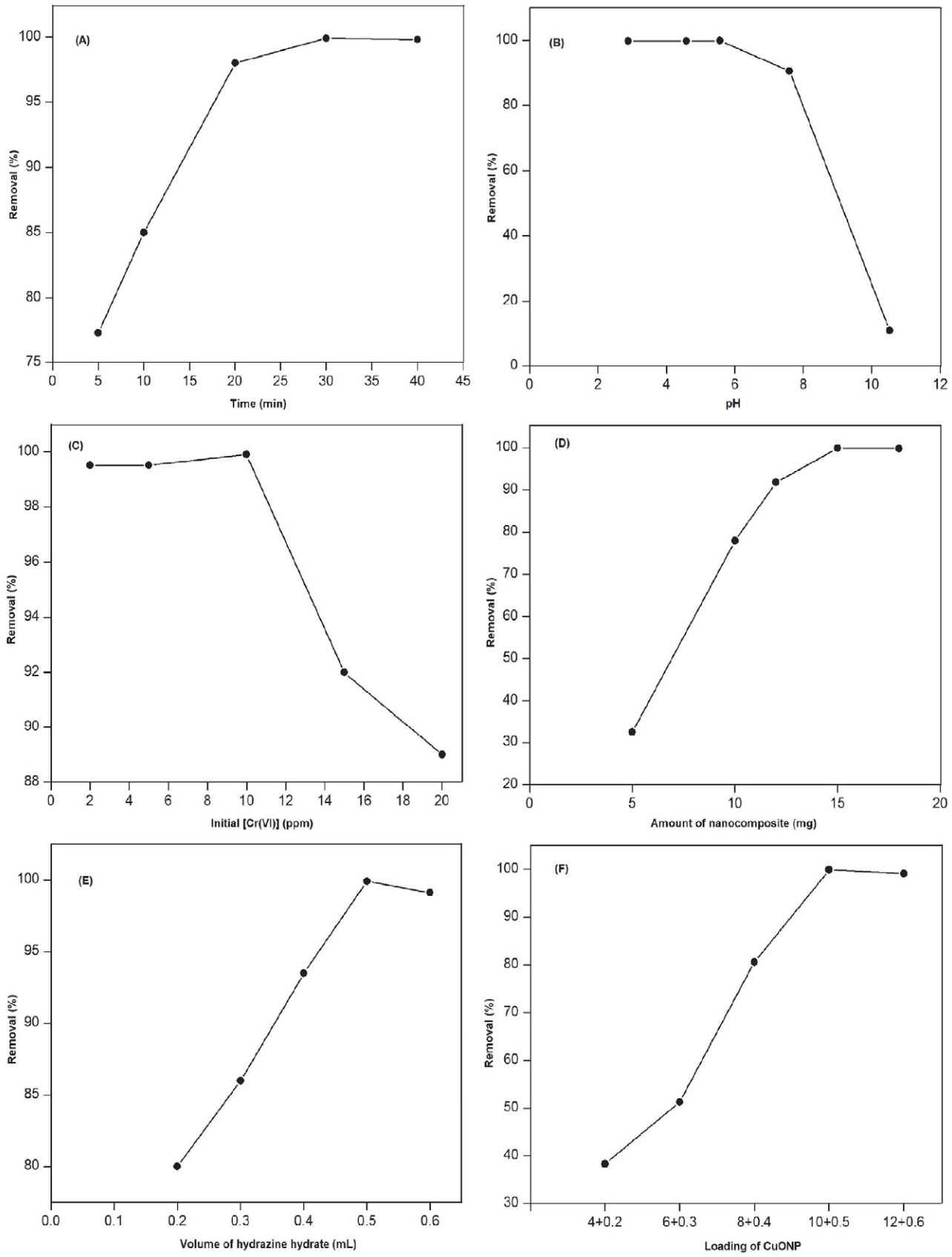

Figure 2: Effect of various factors on the removal of Cr(VI) (A) Duration of experiment, (B) pH (C) Initial Cr(VI) concentration (D) Amount of nano-composite (E) Volume of hydrazine hydrate (F) Loading of CuONP on the support

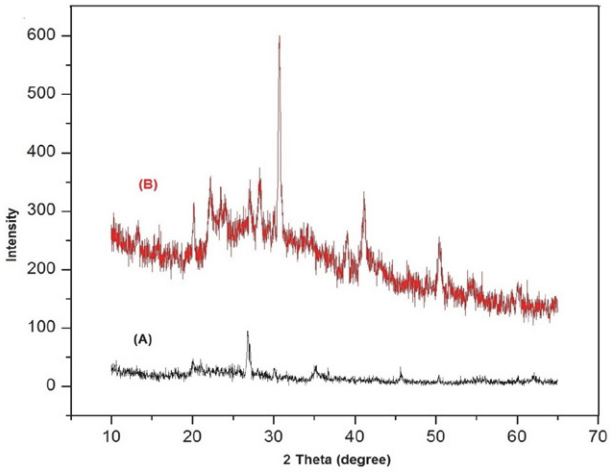

Figure 3: PXRD pattern of (A) pure MMT K10, (B) MMT K10 supported copper oxide nanoparticles

Waals interactions. The EDX study for elemental composition confirmed the presence of the constituent elements O, Si, Mg, Al, and Cu in reduction method. Removal of Cr(VI) was confirmed by taking SEM-EDX of the composite after the treatment of contaminated samples (Figure **4E** and **4F**). The SEM image shows many aggregates of nanoparticles with the adsorbent particles which resulted in a rough surface and porous structure. In EDX study appearance of the extra peak for chromium along with peaks corresponding to O, Si, Al, Cu confirmed the removal of chromium.

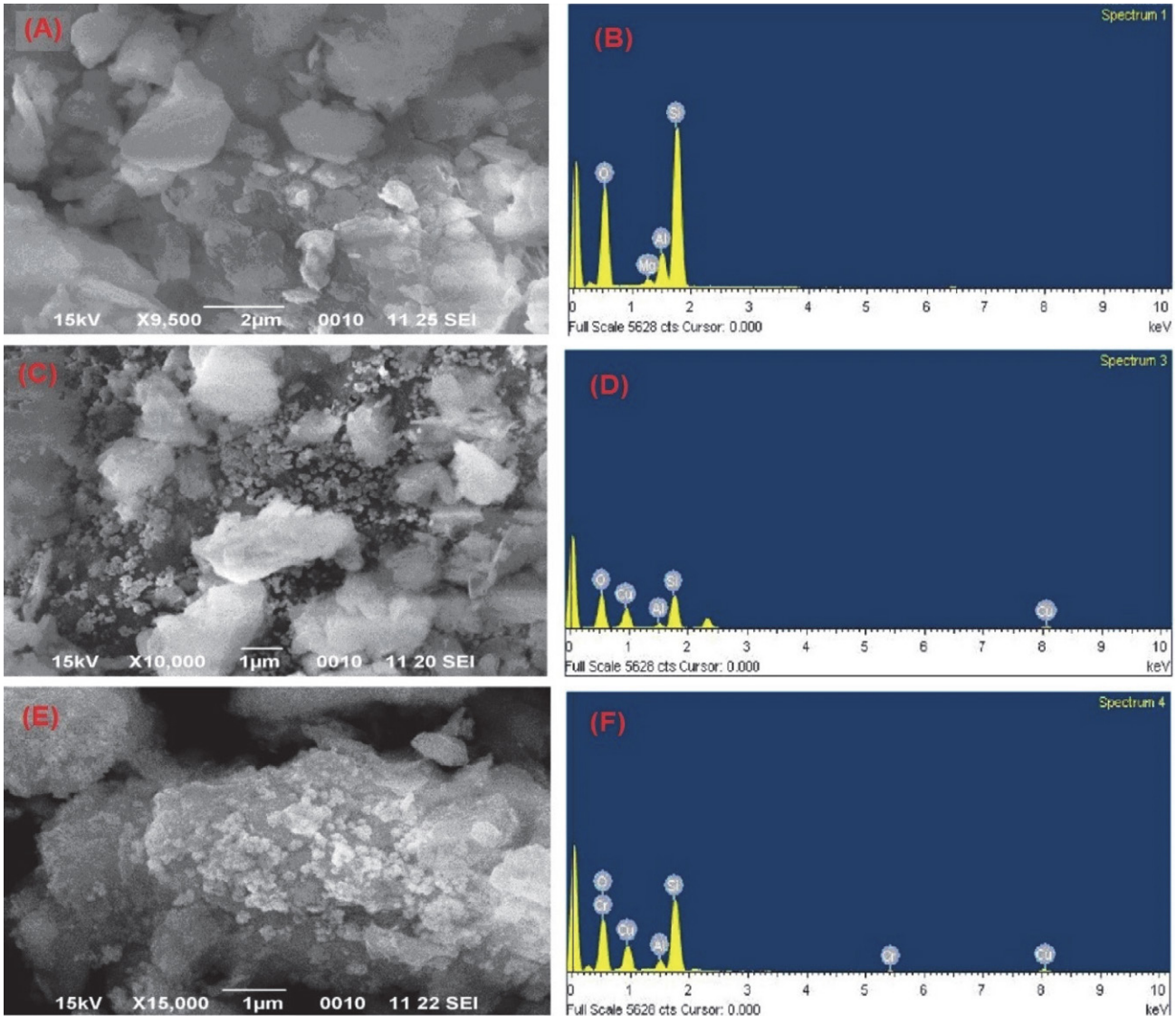

Figure 4: (A) SEM image of pure MMT K10 (B) EDX image of pure MMT K10 (C) SEM image of MMT K10 supported CuONPs (D) EDX image of MMT K10 supported CuONPs (E) SEM image of MMT K10 supported CuONPs after removal of Cr(VI) (F) EDX image of MMT K10 supported CuONPs after removal of Cr(VI)

3. 4. Fourier Transform Infrared Spectroscopy

In FTIR spectra of MMT K10 (Figure **5A**) peaks obtained at 455.60 cm^{-1}, 526.79 cm^{-1} are attributed to Si-O bending and peak at 796.15 cm^{-1} is due to Si-O deformation. Peaks at 1031.90 cm^{-1} and 1210.10 cm^{-1} can be attributed to Si-O stretching. Peak at 920 cm^{-1} is due to (Al, Mg)-OH vibration mode. Peak at 3622.20 cm^{-1} corresponds to O-H stretching at 1367.0 cm^{-1} due to atmospheric CO_2. FTIR spectra of CuONPs supported on MMT K10 (Figure **5B**) shows peak similar to those as obtained in pure MMT K10 with slight shifting in the wave number and intensity. New peak at 613.49 cm^{-1} is observed which is attributed to Cu-O stretching the FTIR spectra confirms loading of CuONPs on the surface of MMT K10.[48–52] FTIR spectra of CuONPs after the removal of chromium (Figure **5C**) shows disappearance of peak at 613.49 cm^{-1} (due to involvement of Cu-O in adsorption of chromium) along with the shifting and decrease in intensity of other peaks compared to MMT K10 supported CuONPs confirms the adsorption of chromium by CuONPs from the solution.

3. 5. Antibacterial Activity of MMT-CuONC Against Gram –ve and Gram +ve Bacteria

The prepared nanoparticles show excellent antibacterial activity against two bacterial strains, one Gram-positive bacterium *Staphylococcus aureus* (ATCC 25323) and one Gram-negative bacterium *Pseudomonas aeruginosa* (ATCC 27853). In all cases, 10.0 mL of 0.1 M $CuSO_4 \cdot 5H_2O$ solution and 0.5 mL of hydrazine hydrates were mixed for the synthesis of CuONPs. It may be mentioned that if the size of nanoparticles is less than that of pore size of the cell membrane of bacteria then they can cross the cell membrane without any hindrance. Control experiments were performed only with MMT K10. It was found that MMT K10 of same concentration shows no capability for antibacterial activity which is clear from Figure 6(A) and 7(A).

The antibacterial activity of CuONPs shows better results against *Pseudomonas aeruginosa* where a maximum zone of inhibition was observed at 39 mm at 100 mg/mL [Figure 6 (B)] in comparison to *Staphylococcus aureus* where a maximum zone of inhibition of 37 mm, at 100 mg/mL [Figure 7 (B)] was observed.

Different molar concentrations of MMT-CuONC are very important in antibacterial activity. Maximum zone of inhibition was observed with different molar concentration of CuONC against *Pseudomonas aeruginosa* while less inhibitory action of CuONC was observed for *Staphylococcus aureus*. On increasing the concentration of CuONC, better inhibitory action can be seen against both Gram-positive *Staphylococcus aureus* and Gram-negative *Pseudomonas aeruginosa* bacteria. Table 2 confirm the results.

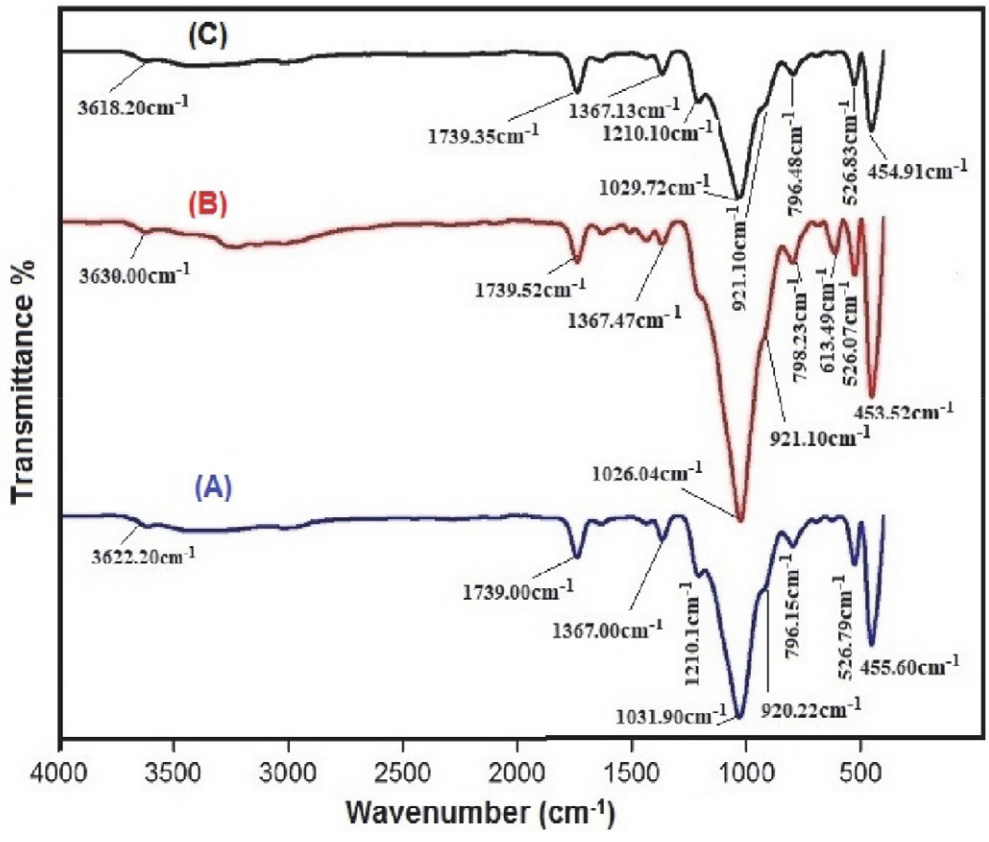

Figure 5: FTIR spectra of (A) MMT K10, (B) loading of CuO nanoparticles, (C) removal of hexavalent chromium

Table 2: Maximum zone of inhibition of different concentration of MMT-CuONC against Gram -ve and Gram +ve bacteria

Microorganisms			CuONPs concentrations (mg/mL)	Maximum Zone of Inhibition (In mm)
Species of Bacteria	**Category of Bacteria**	**Strain**		
Pseudomonas aeruginosa	Gram -ve	ATCC 27853	40	32
			60	34
			80	36
			100	**39**
Staphylococcus aureus	Gram +ve	ATCC 25323	40	18
			60	21
			80	35
			100	**37**

Statistical measurements of zone of inhibition of two bacteria *Pseudomonas aeruginosa* and *Staphylococcus aureus* having standard deviations 35.25 ± 2.98 and 27.75 ± 9.63 was investigated by a two-tail *t*-test of alpha = 0.05 and 6 degree of freedom (df), with a null hypothesis that no differences in the diameters of zone of inhibition for different concentrations of both bacteria where the calculated value of *t* greater than the critical value for *t*, leads to acceptance of the null hypothesis. As mentioned in Table 3, the calculated value of $t = 1.48643622$ which is less than that of the critical value of $t = 2.446911851$ leading to rejection of null hypothesis implying that Gram –ve bacterium *Pseudomonas aeruginosa* and Gram +ve bacterium *Staphylococcus aureus* has different zones of inhibition at different concentrations of CuONC.

Table 3: Statistical measurements of the diameter of zone of inhibition of four samples of *Pseudomonas aeruginosa* and *Staphylococcus aureus* by implying two-tail *t*-test.

***t*-test**	***Pseudomonas aeruginosa***	***Staphylococcus aureus***
Mean	35.25	27.75
Variance	8.916666667	92.91666667
Observations	4	4
Pooled Variance	50.91666667	
Hypothesized Mean Difference	0	
df	6	
t Stat	**1.48643622**	
P(T<=t) one-tail	0.093858141	
t Critical one-tail	1.943180281	
P(T<=t) two-tail	0.187716282	
t Critical two-tail	**2.446911851**	

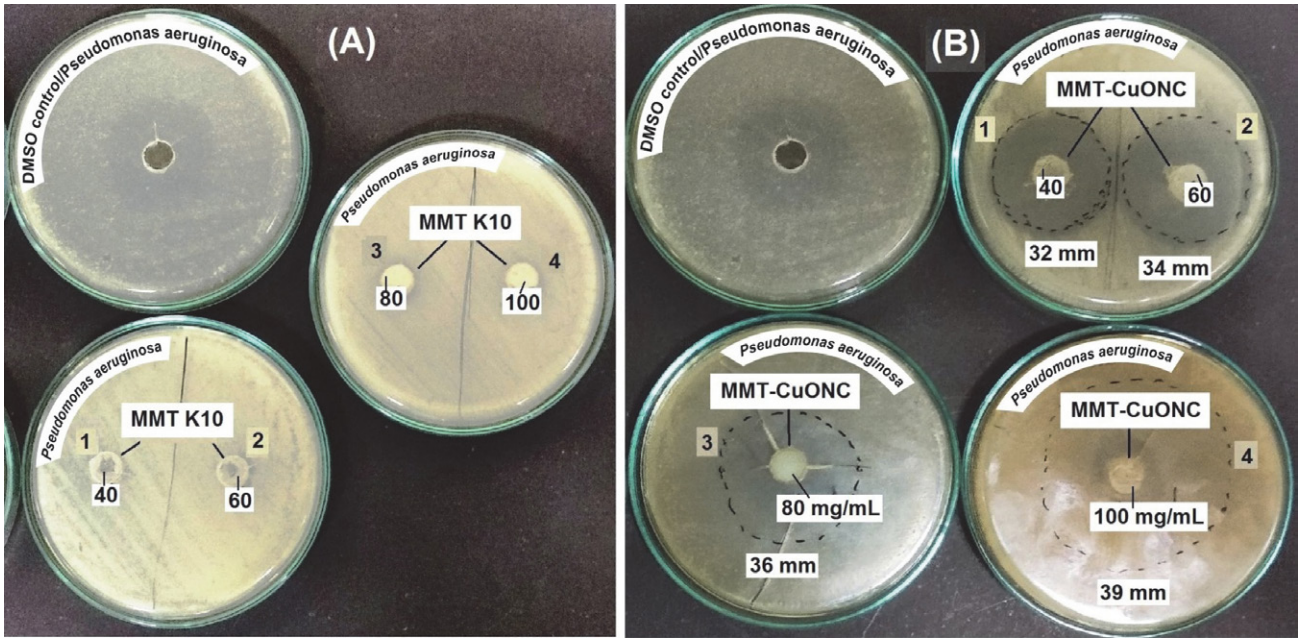

Figure 6: Zone of inhibition of MMT K10 (A) and synthesized MMT supported copper oxide nanoparticles (B) against *Pseudomonas aeruginosa* (Gram negative) at different concentrations (40, 60, 80, 100 mg/mL)

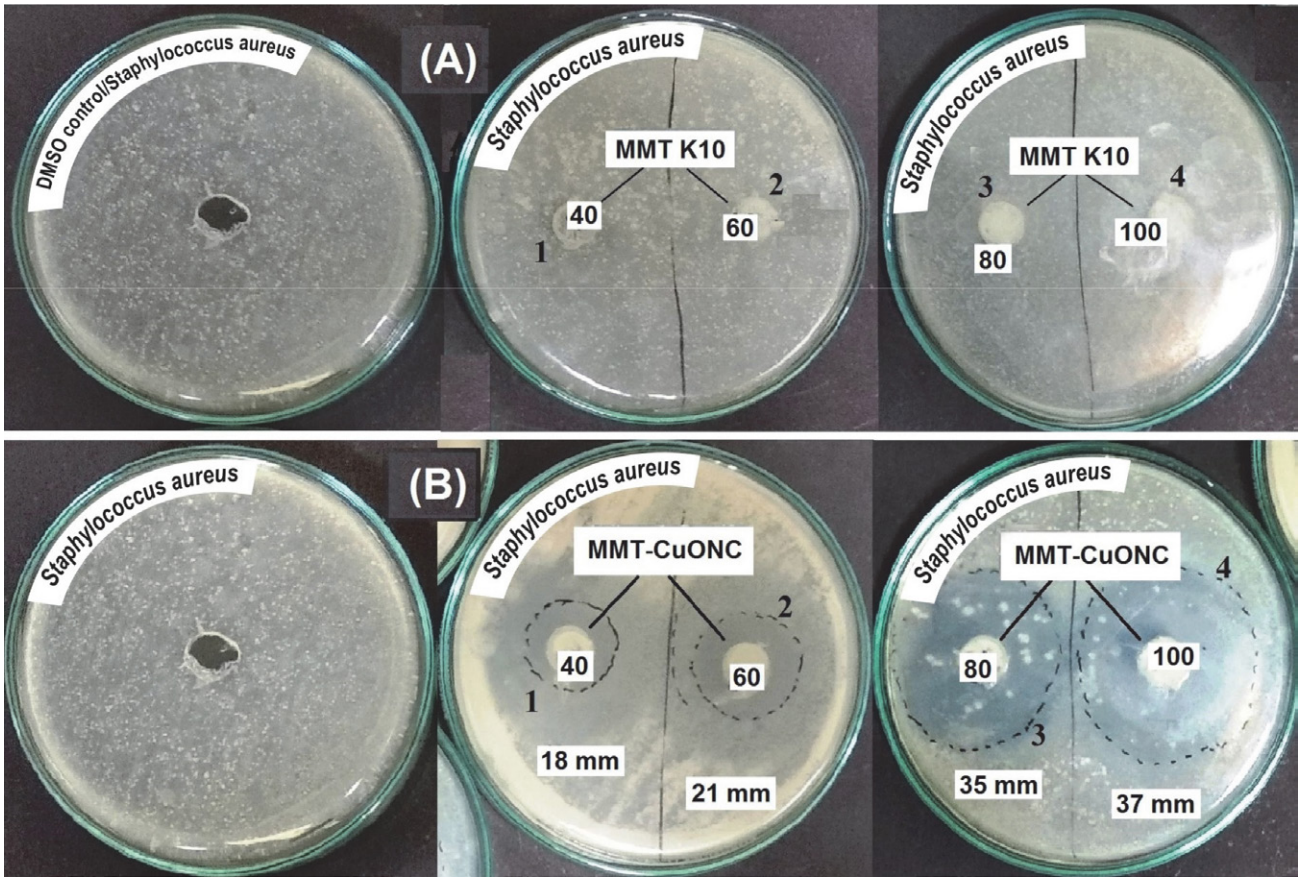

Figure 7: Zone of inhibition of MMT K10 (A) and synthesized MMT supported copper oxide nanoparticles (B) against *Staphylococcus aureus* (Gram positive) at different concentrations (40, 60, 80, 100 mg/mL)

4. Conclusions

In the present study CuONPs, having an average size of 22.9 nm, supported on MMT K10 were synthesized and the prepared nanocomposite was used to remove chromium(VI) from the contaminated water. Antibacterial efficiency of the prepared nanocomposite was also studied against two bacterial strains. It was observed that MMT K10 apart from acting as a stabilizing agent increases the efficiency of CuONC also. Most important observation which to the best of our knowledge has not been reported till now that the synthesized CuONC was able to almost completely (99.9%) remove chromium(VI) from the contaminated water in a very wide pH range of 2.58 to 5.56 and that too within 30 min. Maximum removal of Cr(VI) (99.9%) was obtained at pH 5.56. The nanocomposite showed good antibacterial activity against two bacterial strains, *Staphylococcus aureus* and *Pseudomonas aeruginosa*. 39 mm and 37 mm zones of inhibition at 100 mg/mL were observed in case of *P. aeruginosa* and *S. aureus* respectively. Thus, the prepared nanocomposite has good potential for killing the reported bacterial strains. Moreover, the statistical analysis of two-tail *t*-test also shows that both bacteria have different zone of inhibition for different concentrations of CuONC.

Acknowledgement

Authors thank MNNIT, Prayagraj for XRD, MNIT, BBAU, Lucknow for SEM-EDX and MNIT, Jaipur for FTIR facilities. Author thank U.G.C; New Delhi for the financial support to carry out this work.

5. References

1. J. V. M, R. R, M. Thomas, J. T. Varkey,*Mater. Today Proc.***2019,** *9,* 27–31. **DOI:**10.1016/j.matpr.2019.02.032
2. S. Avudainayagam, M. Megharaj, G. Owens, R. S. Kookana, D. Chittleborough, R. Naidu, *Rev. Environ. Contam. Toxicol.* **2003,** *178,* 53–91. **DOI:**10.1007/0-387-21728-2_3
3. G. López-Téllez, C. E. Barrera-Díaz, P. Balderas-Hernández, G. Roa-Morales, B. Bilyeu, *Chem. Eng. J.* **2011,** *173,* 480–485. **DOI:**10.1016/j.cej.2011.08.018
4. M. Costa, C. B. Klein, *Crit. Rev. Toxicol.***2006,** *36,*155–163. **DOI:**10.1080/10408440500534032
5. Z. Cheng, A. L. K. Tan, Y. Tao, D. Shan, K. E. Ting, X. J. Yin, *Int. J. Photoenergy.***2012,** 1–5. **DOI:***10.1155/2012/608298*
6. E. Sahinkaya, A. Kilic, *Water Res.* **2014,** *50,* 278–286. **DOI:**10.1016/j.watres.2013.12.005
7. J. H. Chen, K. C. Hsu, Y. M. Chang, *Ind. Eng. Chem. Res.*

2013, *52,* 11685–11694. **DOI:**10.1021/ie401233r
8. M. Costa, *Toxicol. Appl. Pharmacol.* **2003,** *188,* 1–5.
9. H. Ma, J. Zhou, L. Hua, F. Cheng, L. Zhou, X. Qiao, *J. Clean. Prod .***2016**. **DOI:**10.1016/j.jclepro.2016.10.193.
10. L. Ben Tahar, M. H. Oueslati, M. J. A. Abualreish, *J. Colloid Interface Sci.* **2018,** *512,* 115–126. **DOI:**10.1016/j.jcis.2017.10.044
11. M. A. Barakat, *Arab. J. Chem.* **2011,** *4,* 361–377. **DOI:**10.1016/j.arabjc.2010.07.019
12. A. S. Dharnaik, P. K. Ghosh, *Environ. Technol.* **2014,** *35,* 2272–2279. **DOI:**10.1080/09593330.2014.902108
13. A. Mnif, I. Bejaoui, M. Mouelhi, B. Hamrouni, *Int. J. Anal. Chem.* **2017,** 1–10. **DOI:**10.1155/2017/7415708
14. A. K. Golder, A. K. Chanda, A. N. Samanta, S. Ray, *Sep. Sci. Technol.* **2007,** *42,*2177–2193. **DOI:**10.1080/01496390701446464
15. Ihsanullah, A. Abbas, A. M. Al-Amer, T. Laoui, M. J. Al-Marri, M. S. Nasser, M. Khraisheh, M. A. Atieh, *Sep. Purif. Technol.* **2016,** *157,* 141–161. **DOI:**10.1016/j.seppur.2015.11.039
16. B. Biškup, B. Subotić, *Sep. Sci. Technol.* **2005,** *39,* 925–940. **DOI:**10.1081/SS-120028454
17. A. B. Moradi, H. M. Conesa, B. H. Robinson, E. Lehmann, A. Kaestner, R. Schulin, *Environ. Pollut.* **2009,** *157,* 2189–2196. **DOI:**10.1016/j.envpol.2009.04.015
18. K. Zare, V. K. Gupta, O. Moradi, A. S. H. Makhlouf, M. Sillanpää, M. N. Nadagouda, H. Sadegh, R. Shahryari-ghoshekandi, A. Pal, Z. Wang, I. Tyagi, M. Kazemi, *J. Nanostructure Chem.* **2015,** *5,* 227–236. **DOI:**10.1007/s40097-015-0158-x
19. S. L. Percival, P. G. Bowler, J. Dolman, *Int. Wound J.* **2007,** *4,* 186–191. **DOI:**10.1111/j.1742-481X.2007.00296.x
20. N. Cioffi, L. Torsi, N. Ditaranto, G. Tantillo, L. Ghibelli, L. Sabbatini, T. Bleve-Zacheo, M. D'Alessio, P. G. Zambonin, E. Traversa, *Chem. Mater.* **2005,** *17,* 5255–5262. **DOI:**10.1021/cm0505244
21. M. Masalha, I. Borovok, R. Schreiber, Y. Aharonowitz, G. Cohen, *J. Bacterio.* **2001,** *183,* 7260–7272. **DOI:**10.1128/JB.183.24.7260-7272.2001
22. V. V. T. Padil, M. Černík, *Int. J. Nanomedicine*, **2013,** *8,* 889–898.
23. A. Azam, A. S. Ahmed, M. Oves, M. S. Khan, S. S. Habib, A. Memic, *Int. J. Nanomedicine,* **2012,** *7,* 6003–6009. **DOI:**10.2147/IJN.S35347
24. D. K. Jena, P. K. Sahoo, *J. App. Pol. Sci.* **2018,** 45968.
25. J. Jain, S. Arora, J. M. Rajwade, P. Omray, S. Khandelwal, K. M. Paknikar, *Mol. Pharm.* **2009,** *6,*1388–1401. **DOI:**10.1021/mp900056g
26. S. Maurya, A. K. Bhardwaj, K. K. Gupta, S. Agarwal, A. Kushwaha, V. Chaturvedi, R. K. Pathak, R. Gopal, K. N. Uttam, A. K. Singh, V. Verma, M. P. Singh, *Cell. Mol. Biol.* **2016,** *62,* 1000131.
27. N. Cioffi, N. Ditaranto, L. Torsi, R. A. Picca, E. De Giglio, L. Sabbatini, L. Novello, G. Tantillo, T. Bleve-Zacheo, P. G. Zambonin, *Anal. Bioanal. Chem.* **2005,** *382,*1912–1918. **DOI:**10.1007/s00216-005-3334-x
28. K. Y. Yoon, J. Hoon Byeon, J. H. Park, J. Hwang, *Sci. Total Environ.* **2007,** *373,*572–575. **DOI:**10.1016/j.scitotenv.2006.11.007
29. K. H. Thompson, C. Orvig, *Science,* **2003**, *300,* 936–939. **DOI:**10.1126/science.1083004
30. M. L. Schilsky, *Pediatr. Transplant,* **2002,** *6,*15–19. **DOI:**10.1034/j.1399-3046.2002.1r069.x
31. O. Mahapatra, M. Bhagat, C. Gopalakrishnan, K. D. Arunachalam, *J. Exp. Nanosci.* **2008,** *3,* 185–193. **DOI:**10.1080/17458080802395460
32. A. Esteban-Cubillo, C. Pecharromán, E. Aguilar, J. Santarén, J. S. Moya,*J. Mater. Sci.* **2006,** *41,*5208–5212. **DOI:**10.1007/s10853-006-0432-x
33. R. Usha, E. Prabu, M. Palaniswamy, C. K. Venil, R. Rajendran, *Glob. J. Biotechnol. Biochem.* **2010,** *5,* 153–160.
34. K. Gopalakrishnan, C. Ramesh, V. Ragunathan, M. Thamilselvan, *Dig. J. Nanomater. Biostructures,* **2012,** *7,* 833–839.
35. M. R. J. Salton, *J. Gen. Microbiol.* **1963**, 30, 223–235. **DOI:**10.1099/00221287-30-2-223
36. T. J. Beveridge, Int. Rev. Cytol, **1981,** *72*, 229–317. **DOI:**10.1016/S0074-7696(08)61198-5
37. T. J. Beveridge, L. L. *Microbiol. Rev.* **1991,** *55*, 684–705. **DOI:**10.1128/mr.55.4.684-705.1991
38. H. Nikaido, T. Nakae, *Adv. Microb. Physiol,***1979**, *20*, 163–250. **DOI:**10.1016/S0065-2911(08)60208-8
39. W. Vollmer, J.V. Holtje, *J. Bacteriol.* **2004**, *186 (18)*, 5978–5987. **DOI:**10.1128/JB.186.18.5978-5987.2004
40. S. Chandra, A. Kumar, P. K. Tomar, *J. Saudi Chem. Soc.* **2014,** *18,* 149–153. **DOI:**10.1016/j.jscs.2011.06.009
41. R. Sivaraj, P. K. S. M. Rahman, P. Rajiv, S. Narendhran, R. Venckatesh, *Spectrochim. Acta – Part A Mol. Biomol. Spectrosc.***2014,** *129,* 255–258. **DOI:**10.1016/j.saa.2014.03.027
42. R. K. Swarnkar, S. C. Singh, R. Gopal, International Conference on Optics and Photonics, **2009,** 1–3.
43. Method 7196A, Chromium hexavalent (colorimetric), http://www3.epa.gov/ epawaste/hazard/testmethods/sw846/pdfs/7196a.pdf. 7196 A1–7196 A6.
44. E. Alzahrani, R. A. Ahmed, *Int. J. Electrochem. Sci.***2016,** *11,* 4712–4723. **DOI:**10.20964/2016.06.83
45. F. W. Harun, E. A. Almadni, E. S. Ali, *Lect. Notes Eng. Comput. Sci.* **2017,** *2,* 606–610.
46. G. M. Raghavendra, J. Jung, D. Kim, J. Seo, *Carbohydr. Polym.* **2017,** *172,* 78–84. **DOI:**10.1016/j.carbpol.2017.04.070
47. I. Muthuvel, B. Krishnakumar, M. Swaminathan,*Indian J. Chem. – Sect. A Inorganic, Phys. Theor. Anal. Chem.* **2012,** *51,* 800–806.
48. P. K. Tandon, R. C. Shukla, S. B. Singh,*Ind. Eng. Chem. Res.* **2013,** *52,*10052–10058. **DOI:**10.1021/ie400702k
49. K. Shameli, M. Mansor Bin Ahmad, Z. Mohsen, W. Z. Yunis, N. A. Ibrahim, A. Rustaiyan, *Int. J. Nanomedicine,* **2011,** *6,* 581–590. **DOI:**10.2147/IJN.S17112
50. A. Azam, A. S. Ahmed, M. Oves, M. Khan, A. Memic, *Int. J. Nanomedicine,* **2012,** *7,*3527–3535.
51. Y. K. Abdel-Monem, S. M. Emam, H. M. Y. Okda, *J. Mater. Sci. Mater. Electron.* **2017,** *28,* 2923–2934. **DOI:**10.1007/s10854-016-5877-3
52. V. K. Gupta, R. Chandra, I. Tyagi, M. Verma,*J. Colloid Nad Inteface Sci.* **2016**, 478, 54–62. **DOI:**10.1016/j.jcis.2016.05.064

Povzetek

Nanodelce bakrovega oksida (CuONPs) na montmorilonitni K10 (MMT K10) osnovi smo pripravili z vključevanjem CuONPs na površino MMT K10 preko redukcije kovinskega prekurzorja s pomočjo hidrazin hidrata. Preučili smo vpliv različnih dejavnikov na učinkovitost odstranjevanje šestvalentnega kroma s pomočjo pripravljenega kompozita. Pod optimalnimi pogoji smo lahko s 15 mg pripravljenega kompozita v 30 min skoraj popolnoma (99.9 %) odstranili šestvalentni krom iz vodne raztopine, ki je vsebovala 10 ppm kroma, v širokem pH območju med 2.88 in 5.56. Sintetiziran MMT K10 – CuONPs kompozit smo okarakterizirali z UV, SEM-EDX, FTIR in XRD. Povprečna velikost kompozitnih delcev je bila 22.9 nm. Antibakterijski potencial pripravljenega kompozita smo preverili z gram-pozitivno bakterijo *Staphylococcus aureus* (ATCC 25323) in gram-negativno bakterijo *Pseudomonas aeruginosa* (ATCC 27853). Ugotovili smo, da pripravljeni kompozit izkazuje močno baktericidno delovanje saj je statistična analiza z uporabo *t*-testa pokazala za oba bakterijska seva različne cone inhibicije pri različnih koncentracijah.